Genome-Scale reconstruction of *Paenarthrobacter aurescens* TC1 metabolic model towards the study of atrazine bioremediation

Shany Ofaim[1,2¥], Raphy Zarecki[1¥], Seema Porob[3], Daniella Gat[3], Tamar Lahav[1], Yechezkel Kashi[2], Radi Aly[1], Hanan Eizenberg[1], Zeev Ronen[3 †] & Shiri Freilich*[†]

[1]Newe Ya'ar Research Center, Agricultural Research Organization, Ramat Yishay, Israel, [2]Faculty of Biotechnology and Food Engineering, Technion-Israel Institute of Technology, Haifa, Israel, [3]Department of Environmental Hydrology & Microbiology, Zuckerberg Institute for Water Research, Jacob Blaustein Institutes for Desert Research, Ben-Gurion University of the Negev, Midreshet Ben-Gurion, 8499000, Israel

[¥]equal contribution

[†] equal contribution

* Corresponding author

email address (in the order of author list): shashany@gmail.com, raphy.zarecki@gmail.com, porob@post.bgu.ac.il, gat.daniella@gmail.com, lahav008@gmail.com, kashi@technion.ac.il, radi@volcani.agri.gov.il, eizenber@volcani.agri.gov.il, zeevrone@bgu.ac.il, shiri.freilich@gmail.com.

ABSTRACT

Atrazine is an herbicide and pollutant of great environmental concern that is naturally biodegraded by microbial communities. *Paenarthrobacter aurescens* TC1 is one of the most studied degraders of this herbicide. Here, we developed a genome scale metabolic model for *P. aurescens* TC1, *i*RZ1176, in order to study the atrazine degradation process and mechanism at organism level. Constraint based flux balance analysis and time dependent simulations were used to explore the bacteria's phenotypic landscape. Simulations led to model based predictions for growth and atrazine degradation efficiency in myriad of media supplemented with different combinations of carbon and nitrogen sources. Simulations aimed at designing media optimized for supporting growth and enhancing degradation, bypassing the need in strain design *via* genetic modifications. Predictions were tested *in vitro* and experimental growth and degradation measurements support and validate the reliability of the model. Model simulations have prioritized degradation and growth enhancement effect of various amino acid and co-factors. The model presented here can potentially serve as a predictive tool towards achieving optimal biodegradation efficiencies and for the development of ecologically friendly solutions for pollutant degradation.

Introduction

Atrazine (2-chloro-4-ethylamino-6-isopropylamino-1,3,5-triazine) is an herbicide and pollutant of great environmental concern. Its residues are found in soil samples decades after it was last applied and were shown to chronically leach into local aquifers[1]. Areas contaminated with hazardous materials, including atrazine, are rapidly increasing worldwide introducing a need in remediation approaches.

49 Bioremediation - an environmental bioprocess in which naturally occurring organisms
50 are used for breaking down hazardous substances into less toxic or non-toxic
51 substances - is increasingly acknowledged as a cost-effective strategy for
52 environmental cleaning[2-4]. Critical environmental bioprocesses are naturally carried
53 out by bacteria and are related to removal of pollutants from water, soil or air[5]. Thus,
54 bacterial bioremediation is widely applied for the degradation of various organic
55 pollutants [6-9] including herbicides[9-13]. Bioremediation may occur naturally or through
56 the stimulating addition of fertilizers, electron acceptors, etc. These amendments
57 encourage the growth of the degrading microbes within the medium or environment
58 in a process termed biostimulation [3,14].
59 One of the well-known atrazine degraders is the gram positive *Paenarthrobacter*
60 *aurescens* TC1[15-19]. *P. aurescense* TC1 is described as nutritionally versatile bacterium
61 that is capable of utilizing a wide array of complex metabolites, including agriculturally
62 used herbicides[4,20,21]. The full hydrolytic pathway for atrazine degradation was
63 reported and described in *P. aurescens* TC1[21]. Moreover, This bacterium was
64 previously reported to biodegrade atrazine much more efficiently than most atrazine
65 degrading bacteria including *Pseudomonas* sp. ADP [22]. Intermediates, created in the
66 degradation process are further metabolized by the organism and can provide sole
67 sources for carbon and nitrogen[18]. While *P.*ADP can only use the hydrolytic products
68 of the ring cleavage as nitrogen but not as carbon; TC1 can use the side groups of
69 atrazine as source for carbon, nitrogen and energy consuming up to 3,000 mg of
70 atrazine per liter [18]. As such, *P. aurescens* TC1 is an ideal candidate for the study of
71 atrazine bioremediation using a genome scale metabolic model reconstruction.

72 Modern tools of genomics, transcriptomics, metabolomics, proteomics, signaling
73 systems and synthetic biology have opened new avenues for biotechnological
74 advances and are increasingly applied for promoting better understanding of complex
75 biological systems. In recent years, constraint based metabolic modelling approaches
76 have become widely used as an *in silico* tool for organism-level phenotyping and the
77 subsequent development of metabolic engineering strategies [23,24]. Generally, such
78 approaches follow four key steps: (1) data acquisition – mainly genome sequencing
79 information, basic cell-physiological and biochemical knowledge and some
80 experimental data on cell growth; (2) model reconstruction - translating data into
81 structured mathematical representation; (3) constraint-based optimization
82 simulations - the prediction of growth rate, substrate uptake rates, and byproduct
83 rates under different growth conditions or following knockout mutations, in the
84 absence of kinetic information[25-31]; and (4) experimental validation. The potential of
85 such models for the investigation of optimal processing is now acknowledged and
86 practiced[5,32-35]. Examples for applicative use include the optimal production or
87 utilization of industrial compounds such as xylose[36], biofuels [37],vitamins [38] and drug
88 development[39]. In bioremediation, genome scale metabolic modeling approaches
89 were applied for the design of *Geobacter sulfurreducens* strain capable of increased
90 electron transfer and a higher Fe(III) respiratory that was beneficial for environmental
91 bioremediation[40]. Application of genome scale metabolic modeling for strain design is
92 often based on the Optknock algorithm [41] and its derivatives which search for the
93 optimal gene knockouts for a desired metabolic production. However, unlike
94 industrial use of engineered strain for enhanced production in monoculture,
95 introduction of exogenous species into natural habitat is far from trivial and hampers

96 the application of modeling approaches towards bioremediation solutions. An
97 alternative strategy is the use of modeling for the design of optimal conditions that
98 will enhance processes (degradation or synthesis) carried by the endogenous
99 community[42]. For example, interactions between *Geobacter* and *Rhodoferax* – a
100 competitor Fe(III)-reducers in anoxic subsurface environments - were captured and
101 described using metabolic modelling and allowed identification of optimal
102 degradation conditions[43]. Models can also predict the benefits of cooperative and
103 commensal interactions to degradation efficiency. Xu *et al* have demonstrate the use
104 of metabolic models for predicting interactions between *P.aurescens* TC1 and
105 endogenous soil species. Exchange metabolites secreted by non-degraders species
106 contribute for enhancing *P.aurescens* TC1 growth and expediting degradation
107 efficiency[44,45]. Here, we directly focused on modeling-based identification of media
108 supplements that can enhance degradation. We describe the process of manual
109 curation of *P.aurescens* TC1 draft metabolic model, its application for predicting
110 growth and atrazine degradation in media containing different carbon and nitrogen
111 sources based on a dynamic (capable of reporting changes over time) and non-
112 dynamic flux based algorithms, and the experimental testing of the predictions.

113

114 **Results**

115 *P.aurescens* TC1 genome scale metabolic network reconstruction

116 The genome of *P.aurescens* TC1 is composed of a circular chromosome of 4.6 Mb
117 coding for 4,222 open reading frames (ORFs) as well as two plasmids, 0.3 Mb each,
118 coding for additional ~600 ORFs[20]. To capture the most comprehensive metabolic

119 capacities encoded in genome and plasmids, a genome-scale metabolic model was
120 reconstructed. To this end, the genome and plasmids were annotated and used to
121 create a draft reconstruction using the Model SEED pipeline[46]. Additional genome
122 annotations of *P.aurescens* TC1 from four established and comprehensive public
123 resources and databases (RAST, KEGG, JGI and UniProt) were then added to the draft
124 network. Model Reactions involved in atrazine degradation pathway and its further
125 conversion into the cellular building blocks isopropylamine and ethylamine were
126 added manually (Fig. 1) based on a detailed reports of the pathway in the specific
127 strain[18,47]. *P.aurescens* TC1 degrades atrazine by hydrolytic dechlorination. The
128 process is catalyzed by triazine hydrolase (TrzN) followed by two hydrolytic
129 deamination reactions catalyzed by hydroxyatrazine hydrolase (AtzB) and N-
130 isopropylammelide isopropylaminohydrolase (AtzC) (reactions rxn06933, rxn03845
131 and rxn03846 in Fig. 1, respectively). These enzymes convert atrazine to cyanuric acid
132 and release the alkylamines ethylamine and isopropylamine. Cyanuric acid
133 accumulates stoichiometrically, whereas the alkylamines are further catabolized into
134 cellular building blocks[21]. Ethylamine and isopropylamine are converted into
135 acetaldehyde and L-alanine (Fig. 1), respectively, and can serve as sole sources of
136 carbon and nitrogen required for growth [18]. Relevant reactions that were missing in
137 the automatic reconstruction were manually added to the model and are shown in
138 Fig. 1. Simulations were carried iteratively to ensure the production of all biomass
139 components under the minimal feasible conditions described in Strong, et al. [18]. The
140 reconstructed metabolic network presented here covers 25% of the ORFs present in
141 the genome and includes 1176 genes, 2541 reactions, out of which 125 are exchange,
142 and 2848 metabolites. The coverage of the genome is similar to those of previously

143 published reconstructed metabolic networks of gram positive bacteria such as *C.*
144 *difficile* or *B. subtilis* with 20% [48,49] and the overall number of reactions is similar to the
145 number of reactions covered by gold standard, updated models of species with similar
146 genome sizes such as *i*JO1366 [50]. A detailed description of the network including the
147 reactions, metabolites, genes, and compartments that comprise the network is
148 provided in Supplemental data 1. The model is also available here as Systems Biology
149 Markup Language (SBML) file [51] in Supplemental data 2. The SBML file can be used
150 with tools such as MATLAB or other SBML compliant software. The minimal media
151 used for simulations are available in Supplemental data 3.
152
153 Validations of *i*RZ1176's *in silico* predictions
154 As previously reported, *P.aurescens* TC1 degrades atrazine and metabolizes its
155 intermediates, isopropylamine and ethylamine. Both can be used as sole carbon and
156 nitrogen sources. Growth simulations confirm that the model captures these reported
157 physiological capacities. Experimental growth measurements verify model
158 simulations and show that atrazine and its degradation products isopropylamine and
159 ethylamine can be used as sole carbon and nitrogen sources for *P. aurscens* TC1 (Fig.
160 2A). Supplementing the medium with glucose enhanced growth both *in silico* and *in*
161 *vitro,* while the addition of ammonia had not shown an effect on growth. This is in
162 accordance with previous work stating that *P.aurescens* TC1 growth is not inhibited
163 by nitrogen sources such as ammonia [22], unlike the inhibition of atrazine degradation
164 in *Pseudomonas sp. strain* ADP in nitrogen rich environments [52].
165 Finally, growth simulations under a gradient of nitrogen *vs*. carbon sources further
166 illustrate that atrazine serves as a good nitrogen source and as a poor carbon source

167 (Fig. 2B). The growth promoting potential of combinations of atrazine with ammonium
168 (NH_4^+) and glucose as nitrogen and/or carbon sources respectively was tested. The
169 effect of nutrient ratio on growth rate was predicted by optimizing the production of
170 biomass across uptake gradients while constraining the fluxes through exchange
171 reactions for carbon and nitrogen sources. As expected, increasing glucose uptake
172 increased the growth rate (Fig. 2B) and the maximal achievable growth rate was much
173 higher with glucose as a carbon source in comparison to atrazine as a sole carbon
174 source. However, atrazine is as equally good nitrogen source as ammonia. This may
175 be endorsed by ammonium as a byproduct of the atrazine degradation process (Fig.
176 1).

177

178 Media modifications effect on *P.* aurescens TC1 growth

179 In addition to glucose, several carbon sources were previously reported to enhance
180 growth of several strains of *Arthrobacter* species in atrazine containing media [21,22,53].
181 To identify additional media modifications that can potentially increase atrazine
182 degradation, we simulated growth in 123 different media combinations, each
183 supplementing the atrazine containing minimal mineral media with a single exchange
184 metabolite. Several sugars, amino acids and dipeptides were predicted to induce
185 enhanced growth (Supplemental data 4). This is in accordance with the previous
186 characterization of *P.aurescens* TC1 as a metabolically versatile species [20,21]. Out of a
187 variety of potential nutritional sources, *Paenarthrobacter* species have been shown to
188 utilize different amino acids in different capacities [54,55]. The three amino acids
189 isoleucine, histidine and methionine are predicted to support growth in high, mediate,

190 and low efficiency, respectively (Supplemental data 4). Dynamic simulations of growth
191 supplementing media with these three amino acids indicated that their effect is media
192 dependent (Fig. 3). Isoleucine has the strongest predicted effect on growth in atrazine
193 containing medium whereas histidine has stronger effect in the same medium without
194 atrazine; methionine has the weakest effect in all media (Fig. 3). *P.aurescens* TC1
195 growth in *in vitro* media corresponding to the media used for the *in silico* simulations
196 were generally in agreement with model's predictions, supporting the superiority of
197 isoleucine over histidine in atrazine supplemented media but not in the atrazine
198 deficient medium (Fig. 3). Supplementing media with methionine showed a weaker
199 effect on growth in comparison to the other two amino acids tested, agreeing with its
200 weak effect in simulations. This is also in agreement with a recent work by Deutch [55]
201 showing that whereas isoleucine and histidine serve as potential nitrogen and/or
202 carbon sources of *P.aurescens* TC1, methionine does not serve as a growth supporter.
203 Like atrazine, amino acids can potentially serve as both carbon and nitrogen source.
204 Considering C:N ratio as an indicator of growth support potential, isoleucine and
205 histidine have a ratio of 6:1 and 6:3, respectively, whereas methionine, having no
206 growth promoting effect has a ratio of 5:1 (Supplemental data 4). Other amino acids
207 with 5:1 or 5:3 C:N ratio like proline and serine, respectively, are also predicted to be
208 an efficient supporters of growth, similar to isoleucine (Supplemental data 4). Thus,
209 the growth effect of atrazine cannot be predicted merely based on C:N ratio.
210

211 Media modifications effect on atrazine degradation

212 Following the validation of the model predictions for growth capacities, we directly
213 evaluated atrazine degradation in different media conditions. To this end, we applied

214 Flux variability analysis (FVA), allowing the identification of the ranges of flux
215 variability that are possible within a given media[56]. Once the biomass flux was
216 maximized, we estimated the rate of atrazine degradation according to the relevant
217 flux of interest (for example, phosphate). The simulation of atrazine degradation over
218 time was in a medium that contains atrazine as a sole carbon and nitrogen source *vs*.
219 modified media sets (see Methods). Atrazine degradation was estimated according to
220 the amount of atrazine left in the media following each time cycle. Simulations
221 showed that supplementing the media with glucose not only enhances growth (Fig. 2)
222 but also induced an enhancement of atrazine consumption. Predictions were
223 confirmed by experimental validation (Fig. 4).
224 Finally, the addition of phosphate, a main element in fertilizers, to soils has been
225 reported to have a significant effect on the degradation of herbicides. For instance, its
226 addition was shown to effect soil bacteria's degradation activity including a reported
227 effect on *Arthrobacter* sp. HB-5, a close relative of *P.aurescens* TC1[57]. Phosphate has
228 been previously shown to accelerate atrazine degradation[3]. To test the effect of
229 phosphate, we used the model to simulate growth and atrazine degradation in high
230 or limited phosphate conditions. In accordance with these reports, simulations
231 showed similar trends, which were confirmed by experimental results. These indicate
232 an effect of phosphate concentrations *on P. aurescens* TC1 growth (Supplemental data
233 5) and atrazine degradation (Fig. 4).
234

235 **Discussion**

236 The accumulation and persistence of herbicides and their intermediates in soil and
237 drinking water has long been suggested to be disruptive, imposing a need for effective

238 strategies for their degradation and removal [58]. Bioremediation is a widely applied
239 approach for the degradation of herbicides including atrazine [9-13]. Here, we
240 reconstructed a genome scale metabolic model, *i*RZ1176, of *P. aurescnes* TC1, a well-
241 studied atrazine degrader, in order to use the *in silico* simulations for predicting
242 optimal media to support its growth and atrazine degradation activity. The *in silico*
243 simulations were carried on an array of minimal media using atrazine and its interim
244 degradation products as alternative sole carbon and nitrogen sources supplemented
245 by potential enhancers. The simulations suggested a group of metabolites promoting
246 the increase in biomass yield including sugars, amino acids and dipeptides. We
247 hypothesize that the introduction of such an efficient carbon source leads to an
248 increase in biomass and a subsequent increase in the degradation activity. Simulations
249 were confirmed by *in vitro* experimental validation. This genome scale reconstruction
250 may be used for further experimenting and the gain of new biological knowledge of
251 this metabolically versatile bacteria.
252 While the metabolic modeling approach presented here was demonstrated useful for
253 generating predictions, its limitations should be acknowledged. First, model
254 construction relies on automatic protocols and publically free genomic information.
255 Biomass composition and energy maintenance requirements are hence
256 approximations [46,48]. Second, data used to construct the model is eclectic and
257 annotations were gathered from numerous databases. The lack of data
258 standardization has led to many overlaps and misnomers resulting in draft models
259 containing massive gaps. The lion share of the gap filling and network improvement
260 processes are still done manually due to the differences in data description and
261 cataloging in the different databases. As technology and standardization advance, the

262 process of constructing a metabolic model able to produce testable predictions will
263 be faster and have greater accuracy. Despite relying on genomic data and a growth
264 approximation, resulting predictions can successfully capture the relative effect of
265 different media complements on growth and atrazine degradation. Accuracy of
266 predictions is likely to be significantly improved by the addition of other layers of
267 information including metabolomics, transcriptomics and reaction kinetics. These
268 additional layers of information will allow imposing additional constrains on the
269 internal and external fluxes, as well as an accurate description of the biomass
270 composition specific to this strain. Continuation of the manual curation process, also
271 based on added transcription information, is likely to improve the performances of
272 future versions.
273 Overall, we describe the construction of a mathematical stoichiometric metabolic
274 model of *Paenarthrobacter aurescens* TC1 (*i*RZ1176), allowing simulating its
275 degradation activity. Simulations were used to predict growth and degradation
276 following media modifications such as high/low phosphate content and the addition
277 of variety of amino acids and carbon source to the standard minimal R medium. Effects
278 of such media were observed experimentally to effect atrazine degradation. The
279 simulations go beyond the C:N ratio of media components and take into account the
280 complement of reactions and stoichiometric complexity of cellular processes and may
281 be used to further study this versatile organism for the design of improved
282 degradation strategies in soil. Additionally, we demonstrate that through using
283 metabolic time dependent simulations, an optimal range of nutrient augmentation
284 may also be planned. Though soil communities are complex in terms of their
285 composition and microbial consortia dynamics, in a recent study we demonstrated the

286 usefulness of modeling approaches for deciphering metabolic complexities[44], pointing
287 at the future potential of modeling approaches. Despite the complexity of soil
288 communities, supplementing soil with carbon sources is long known to induce a
289 change in microbial structure and function. A predictive tool such as the presented
290 model is a first step towards designing optimal degradation efficiencies that can be
291 further tested in the field. The integration of species-specific models together with
292 community approaches is likely to contribute to our understanding of biodegradation
293 processes in natural environments and promote the development of bioaugmentation
294 and biostimulation strategies.
295
296 **Methods**
297 Reconstruction and curation of the *P. aurescens* TC1 metabolic model
298 An initial draft model of *P. aurescens* TC1 was reconstructed as described in Henry, et
299 al. [46]. Briefly, the complete genome sequence of *P. aurescens* TC1 was retrieved from
300 NCBI (GenBank accession ids. NC_008711 including NC_008711.1 NC_008712.1, and
301 NC_008713.1 – chromosome and two plasmids, respectively), uploaded into RAST [59],
302 spliced into genes and annotated. RAST annotations were put through the Model SEED
303 pipeline [46] and an initial metabolic network reconstruction was obtained. This initial
304 reconstruction contained a list of reactions classified as exchange, transport, and
305 cytosolic as well as a list of all relevant metabolites and a biomass reaction. Based on
306 taxonomy, the gram positive biomass reaction was specified in the process of draft
307 reconstructions using Model SEED and KBase pipelines. The composition of the
308 biomass reaction summarizes the fractional contribution of a generalized microbial
309 biomass precursors (e.g., amino acids and lipids) to the synthesis of a new cell and is

310 similar to the previously published genome scale reconstruction of *B.Subtilis*[48].
311 Unspecified non-metabolic consuming processes in the cell were defined as ATP
312 maintenance and set similarly to [48]. Missing reactions were filled through an automatic
313 gap-filling procedure, using default (optimal) media options [46]. Manual curation
314 procedures were carried to adapt model performances to reported physiological
315 capacities. Simulation conditions were modified to reflect experimentally validated
316 minimal media alternatives that support growth of *P.* aurescnes TC1 [18].
317 Curation procedures were carried iteratively versus growth simulations to ensure the
318 production of all biomass components in Minimal Mineral Media (MMM: K^+, Mn^{2+},
319 CO2, Zn^{2+}, SO_4^-, Cu^{2+}, Ca^{2+}, HPO_4^{2-}, Mg^{2+}, Fe^{2+}, Cl^-), supplemented by alternative carbon
320 and nitrogen sources including atrazine, ethylamine, isopropylamine, ammonia,
321 glucose and selected amino acids. As part of the curation process, the hydrolytic
322 pathway of atrazine degradation was *a priori* added to the model based on previously
323 published biochemical evidence [18]. Reaction directionality was assigned based on the
324 KEGG database. Errors in reaction reversibility and elemental balance were manually
325 identified and corrected according to literature and/or available databases. The model
326 is available in SBML format and as excel sheet (Supplemental data 1 & 2). The minimal
327 media used for simulations are available in Supplemental data 3.
328
329 <u>Flux balance analyses simulations and dynamic, time dependent simulations</u>
330 Flux distributions in the metabolic model were determined using Flux Balance Analysis
331 (FBA) [60-62]. Briefly, a metabolic model includes a network that is described as a
332 stoichiometric matrix $\mathbf{S}_{m \times n}$, where m represents the number of metabolites and n the
333 number of reactions in the model. In the assumed pseudo-steady-state, internal

334 metabolites concentrations and fluxes are assumed to be constant. The model can be
335 represented as: $\mathbf{S} \times v = 0$, where vector v signifies the fluxes through the internal
336 reactions. As the number of reactions (*n*) typically exceeds the number of metabolites
337 (*m*), the system is under-determined. In order to get a feasible solution space, linear
338 programming (LP), subject to mass balance preservation and flux constraints, was
339 used by introducing an optimization problem. Here, model growth was maximized by
340 maximizing its biomass reaction, which was used as objective function. Specific fluxes
341 for metabolites consumption and secretion were determined following fixation of the
342 respective biomass reaction to its maximal value and then using Flux Variability
343 Analysis (FVA)[56], a linear programming method to find the minimal amount of
344 metabolites needed to produce a preset amount of biomass. Dynamic modeling was
345 used for the prediction of the profile of consuming metabolites typical to the biomass
346 increase of *P. aurescens* TC1 and atrazine degradation across time. To this end, we
347 simulated the behavior of our metabolic model across time. This was done as
348 described in [44] and illustrated in Supplemental data 5, based on concepts defined in
349 [63]. Briefly, the model works under the following assumptions: (1) A finite start amount
350 of media components is available; (2) A maximal amount of uptake a single cell can
351 acquire from the media in a given time point is defined (the lower bound of the
352 exchange reaction value); (3) New substrate concentrations in time t, are determined
353 by the predicted substrate concentration for the previous step augmented with any
354 additional substrates provided or consumed in the current iteration. The maximum
355 uptake was set to a ratio of up to 1 unit of each metabolite available in the media; (4)
356 After each time tick, the biomass amount was updated according to the flux amount
357 of the biomass reaction in the model at this time tick. As biomass production rate

358 serves as a proxy for the size of the population in the simulated environment and
359 substrate uptake/secretion is mainly affected by to population size, the model was
360 used to evaluate the actual substrate uptake/secretion and growth rate given the
361 supplied media across time. Simulations were carried until reaching a state where
362 time cycles did not lead to an increase in biomass. Initial concentration values for all
363 metabolites were set to a fixed amount of 50 units (represented as the initial lower
364 bounds, LB, of the exchange reactions). Simulation parameters and defaults are
365 available in Supplemental data 3. Starting with one bacterium, the flux balance model
366 was used to predict the uptake of phosphate, sulfate, carbon and nitrogen sources
367 (*i.e.* atrazine and glucose) by *P. aurescens* TC1 across time.
368 All model simulations were done on an Intel i7 quad-core server with 32GB of
369 memory, running Linux. The development programming language of our simulators
370 was JAVA, and our linear programming software was IBM CPLEX. Surface plots were
371 created using the MATLAB 2019a (MathWorks, Inc., Natick, Massachusetts, United
372 States). Pathway maps were created using Escher maps[64].

373

374 <u>*In vitro* bacterial growth conditions and chemical analysis</u>

375 *P.aurescens* TC1 (ATCC BAA-1386™) was grown on R medium (based on ATCC 2662 R)
376 plates with glucose (0.2%) and atrazine (30 mg/l, Agan Adama -Ashdod, Israel Israel)
377 as sole nitrogen. Stock cultures were maintained in glycerol at -80°C. Cultures were
378 resuscitated on R medium agar plates (1.5% Difco bacto™) and were used as starter
379 colonies for liquid medium growth experiments. The growth of *P.aurescens* TC1 was
380 tested in R media supplemented with different combinations of carbon and nitrogen

381 sources, including Glucose (0.2%), Atrazine (30 mg/l, Agan Adama -Ashdod, Israel),
382 ammonium chloride (37 mg/l), Ethylamine and Isopropylamine (31.1 and 40.8 mg/l,
383 Sigma-Aldrich -Rehovot, Israel) and the amino acids Histidine, Isoleucine and
384 Methionine (36, 92 and 103 mg/l respectively). Concentrations of amino acids,
385 ethylamine and Isopropylamine were calculated to provide the same nitrogen content
386 as the atrazine. In addition to the carbon and nitrogen sources, growth in media
387 supplemented by atrazine and atrazine together with glucose was tested under two
388 phosphate concentrations (K_2HPO_4 in 0.45 and 0.045 g/l). Each substrate was added
389 to sterile R medium and bacteria was grown in triplicate 250ml flasks incubated in
390 30°C with shaking in the dark. One flask contained only R medium and was used as
391 control. A 200 ul sample was taken from each flask every 8 hours for measurement of
392 OD in microplate reader (520nm, Infinite® 200 PRO Tecan, Männedorf Switzerland)
393 and 1 ml was taken to study atrazine degradation rate using HPLC. The HPLC analysis
394 was performed with Agilent 1100 HPLC (Waldbronn Germany) equipped with a DAD
395 detector. Samples were separated on Kinetex C18 column (Phenomenex Torrance, CA)
396 and the mobile phase consisted of 70% methanol flowing at 1 ml/min. Detection and
397 quantitation of atrazine was done at 240 nm with detection limit of 0.1 mg/l. Total
398 duration of each growth experiment was between 152 to 168 hours.

399

400 **References**

401 1 Abubucker, S. *et al.* Metabolic reconstruction for metagenomic data and its
402 application to the human microbiome. *PLoS Comput Biol* **8**, e1002358,
403 doi:10.1371/journal.pcbi.1002358 (2012).
404 2 Kastner, M. & Miltner, A. Application of compost for effective bioremediation of
405 organic contaminants and pollutants in soil. *Appl Microbiol Biotechnol* **100**, 3433-
406 3449, doi:10.1007/s00253-016-7378-y (2016).

3 Kanissery, R. G. & Sims, G. K. Biostimulation for the Enhanced Degradation of Herbicides in Soil. *Applied and Environmental Soil Science* **2011**, 10, doi:10.1155/2011/843450 (2011).

4 Viegas, C. A. *et al.* Evaluating formulation and storage of Arthrobacter aurescens strain TC1 as a bioremediation tool for terbuthylazine contaminated soils: Efficacy on abatement of aquatic ecotoxicity. *Sci Total Environ* **668**, 714-722, doi:10.1016/j.scitotenv.2019.02.355 (2019).

5 Perez-Garcia, O., Lear, G. & Singhal, N. Metabolic Network Modeling of Microbial Interactions in Natural and Engineered Environmental Systems. *Front Microbiol* **7**, 673, doi:10.3389/fmicb.2016.00673 (2016).

6 Nilsson, T., Rova, M. & Smedja Backlund, A. Microbial metabolism of oxochlorates: a bioenergetic perspective. *Biochim Biophys Acta* **1827**, 189-197, doi:10.1016/j.bbabio.2012.06.010 (2013).

7 Mani, D. & Kumar, C. Biotechnological advances in bioremediation of heavy metals contaminated ecosystems: an overview with special reference to phytoremediation. *International Journal of Environmental Science and Technology* **11**, 843-872, doi:10.1007/s13762-013-0299-8 (2013).

8 Shah, J. & Dahanukar, N. Bioremediation of organometallic compounds by bacterial degradation. *Indian J Microbiol* **52**, 300-304, doi:10.1007/s12088-011-0223-1 (2012).

9 Megharaj, M., Ramakrishnan, B., Venkateswarlu, K., Sethunathan, N. & Naidu, R. Bioremediation approaches for organic pollutants: a critical perspective. *Environ Int* **37**, 1362-1375, doi:10.1016/j.envint.2011.06.003 (2011).

10 Nousiainen, A. O. *et al.* Bioremediation strategies for removal of residual atrazine in the boreal groundwater zone. *Appl Microbiol Biotechnol* **99**, 10249-10259, doi:10.1007/s00253-015-6828-2 (2015).

11 Sagarkar, S. *et al.* Soil mesocosm studies on atrazine bioremediation. *J Environ Manage* **139**, 208-216, doi:10.1016/j.jenvman.2014.02.016 (2014).

12 Fan, X. & Song, F. Bioremediation of atrazine: recent advances and promises. *Journal of Soils and Sediments* **14**, 1727-1737, doi:10.1007/s11368-014-0921-5 (2014).

13 Singh, B. & Singh, K. Microbial degradation of herbicides. *Crit Rev Microbiol* **42**, 245-261, doi:10.3109/1040841X.2014.929564 (2016).

14 Adams, G. O., Fufeyin, P. T., Okoro, S. E. & Ehinomen, I. Bioremediation, biostimulation and bioaugmention: a review. *International Journal of Environmental Bioremediation & Biodegradation* **3**, 28-39 (2015).

15 Wang, Q. & Xie, S. Isolation and characterization of a high-efficiency soil atrazine-degrading Arthrobacter sp. strain. *International Biodeterioration & Biodegradation* **71**, 61-66, doi:10.1016/j.ibiod.2012.04.005 (2012).

16 Fang, H., Lian, J., Wang, H., Cai, L. & Yu, Y. Exploring bacterial community structure and function associated with atrazine biodegradation in repeatedly treated soils. *Journal of hazardous materials* **286**, 457-465, doi:10.1016/j.jhazmat.2015.01.006 (2015).

17 Zhang, Y. *et al.* Metabolic ability and individual characteristics of an atrazine-degrading consortium DNC5. *J Hazard Mater* **237-238**, 376-381, doi:10.1016/j.jhazmat.2012.08.047 (2012).

18 Strong, L. C., Rosendahl, C., Johnson, G., Sadowsky, M. J. & Wackett, L. P. Arthrobacter aurescens TC1 metabolizes diverse s-triazine ring compounds. *Appl Environ Microbiol* **68**, 5973-5980 (2002).

19 Sagarkar, S. *et al.* Monitoring bioremediation of atrazine in soil microcosms using molecular tools. *Environ Pollut* **172**, 108-115, doi:10.1016/j.envpol.2012.07.048 (2013).

20 Mongodin, E. F. *et al.* Secrets of soil survival revealed by the genome sequence of Arthrobacter aurescens TC1. *PLoS genetics* **2**, e214, doi:10.1371/journal.pgen.0020214 (2006).
21 Deutch, C. E., Bui, A. P. & Ho, T. Growth of Paenarthrobacter aurescens strain TC1 on atrazine and isopropylamine during osmotic stress. *Annals of Microbiology* **68**, 569-577, doi:10.1007/s13213-018-1364-9 (2018).
22 Silva, V. P. *et al.* Evaluation of Arthrobacter aurescens Strain TC1 as Bioaugmentation Bacterium in Soils Contaminated with the Herbicidal Substance Terbuthylazine. *PloS one* **10**, e0144978 (2015).
23 Xu, C. *et al.* Genome-scale metabolic model in guiding metabolic engineering of microbial improvement. *Appl Microbiol Biotechnol* **97**, 519-539, doi:10.1007/s00253-012-4543-9 (2013).
24 Contador, C. A., Rodriguez, V., Andrews, B. A. & Asenjo, J. A. Genome-scale reconstruction of Salinispora tropica CNB-440 metabolism to study strain-specific adaptation. *Antonie Van Leeuwenhoek* **108**, 1075-1090, doi:10.1007/s10482-015-0561-9 (2015).
25 Mahadevan, R. & Lovley, D. R. The degree of redundancy in metabolic genes is linked to mode of metabolism. *Biophys J* **94**, 1216-1220, doi:10.1529/biophysj.107.118414 (2008).
26 Mahadevan, R. *et al.* Characterization of metabolism in the Fe(III)-reducing organism Geobacter sulfurreducens by constraint-based modeling. *Appl Environ Microbiol* **72**, 1558-1568, doi:10.1128/AEM.72.2.1558-1568.2006 (2006).
27 Oberhardt, M. A. *et al.* Harnessing the landscape of microbial culture media to predict new organism-media pairings. *Nat Commun* **6**, 8493, doi:10.1038/ncomms9493 (2015).
28 Lee, J., Yun, H., Feist, A. M., Palsson, B. Ø. & Lee, S. Y. Genome-scale reconstruction and in silico analysis of the Clostridium acetobutylicum ATCC 824 metabolic network. *Appl Microbiol Biotechnol* **80**, doi:10.1007/s00253-008-1654-4 (2008).
29 Thiele, I., Vo, T. D., Price, N. D. & Palsson, B. O. Expanded metabolic reconstruction of Helicobacter pylori (iIT341 GSM/GPR): an in silico genome-scale characterization of single- and double-deletion mutants. *J Bacteriol* **187**, 5818-5830, doi:10.1128/JB.187.16.5818-5830.2005 (2005).
30 Price, N. D., Papin, J. A., Schilling, C. H. & Palsson, B. O. Genome-scale microbial in silico models: the constraints-based approach. *Trends Biotechnol* **21**, 162-169, doi:10.1016/S0167-7799(03)00030-1 (2003).
31 Reed, J. L., Vo, T. D., Schilling, C. H. & Palsson, B. O. An expanded genome-scale model of Escherichia coli K-12 (iJR904 GSM/GPR). *Genome Biol* **4**, R54, doi:10.1186/gb-2003-4-9-r54 (2003).
32 Fang, Y. *et al.* Direct coupling of a genome-scale microbial in silico model and a groundwater reactive transport model. *J Contam Hydrol* **122**, 96-103, doi:10.1016/j.jconhyd.2010.11.007 (2011).
33 Zomorrodi, A. R. & Segre, D. Synthetic Ecology of Microbes: Mathematical Models and Applications. *J Mol Biol* **428**, 837-861, doi:10.1016/j.jmb.2015.10.019 (2016).
34 Biswas, K., Paul, D. & Sinha, S. N. Biological Agents of Bioremediation: A Concise Review. *Microbiology* **1**, 39-43 (2015).
35 Henson, M. A. Genome-scale modelling of microbial metabolism with temporal and spatial resolution. *Biochem Soc Trans* **43**, 1164-1171, doi:10.1042/BST20150146 (2015).
36 Cordova, L. T., Long, C. P., Venkataramanan, K. P. & Antoniewicz, M. R. Complete genome sequence, metabolic model construction and phenotypic characterization of

Geobacillus LC300, an extremely thermophilic, fast growing, xylose-utilizing bacterium. *Metab Eng* **32**, 74-81, doi:10.1016/j.ymben.2015.09.009 (2015).

37 de la Torre, A. *et al.* Genome-scale metabolic reconstructions and theoretical investigation of methane conversion in Methylomicrobium buryatense strain 5G(B1). *Microb Cell Fact* **14**, 188, doi:10.1186/s12934-015-0377-3 (2015).

38 Zou, W. *et al.* Reconstruction and analysis of a genome-scale metabolic model of the vitamin C producing industrial strain Ketogulonicigenium vulgare WSH-001. *J Biotechnol* **161**, 42-48, doi:10.1016/j.jbiotec.2012.05.015 (2012).

39 Pacheco, M. P., Bintener, T. & Sauter, T. Towards the network-based prediction of repurposed drugs using patient-specific metabolic models. *EBioMedicine*, doi:10.1016/j.ebiom.2019.04.017 (2019).

40 Izallalen, M. *et al.* Geobacter sulfurreducens strain engineered for increased rates of respiration. *Metab Eng* **10**, 267-275, doi:10.1016/j.ymben.2008.06.005 (2008).

41 Burgard, A. P., Pharkya, P. & Maranas, C. D. Optknock: a bilevel programming framework for identifying gene knockout strategies for microbial strain optimization. *Biotechnol Bioeng* **84**, 647-657, doi:10.1002/bit.10803 (2003).

42 Ang, K. S., Lakshmanan, M., Lee, N. R. & Lee, D. Y. Metabolic Modeling of Microbial Community Interactions for Health, Environmental and Biotechnological Applications. *Curr Genomics* **19**, 712-722, doi:10.2174/1389202919666180911144055 (2018).

43 Zhuang, K. *et al.* Genome-scale dynamic modeling of the competition between Rhodoferax and Geobacter in anoxic subsurface environments. *The ISME journal* **5**, 305-316, doi:10.1038/ismej.2010.117 (2011).

44 Xu, X. *et al.* Modeling microbial communities from atrazine contaminated soils promotes the development of biostimulation solutions. *The ISME journal* **13**, 494-508, doi:10.1038/s41396-018-0288-5 (2019).

45 Faust, K. Microbial Consortium Design Benefits from Metabolic Modeling. *Trends Biotechnol* **37**, 123-125, doi:10.1016/j.tibtech.2018.11.004 (2019).

46 Henry, C. S. *et al.* High-throughput generation, optimization and analysis of genome-scale metabolic models. *Nature biotechnology* **28**, 977-982, doi:10.1038/nbt.1672 (2010).

47 Kundu, K. *et al.* Defining lower limits of biodegradation: atrazine degradation regulated by mass transfer and maintenance demand in Arthrobacter aurescens TC1. *The ISME journal*, doi:10.1038/s41396-019-0430-z (2019).

48 Oh, Y. K., Palsson, B. O., Park, S. M., Schilling, C. H. & Mahadevan, R. Genome-scale reconstruction of metabolic network in Bacillus subtilis based on high-throughput phenotyping and gene essentiality data. *The Journal of biological chemistry* **282**, 28791-28799, doi:10.1074/jbc.M703759200 (2007).

49 Larocque, M., Chenard, T. & Najmanovich, R. A curated C. difficile strain 630 metabolic network: prediction of essential targets and inhibitors. *BMC systems biology* **8**, 117, doi:10.1186/s12918-014-0117-z (2014).

50 Orth, J. D. *et al.* A comprehensive genome-scale reconstruction of Escherichia coli metabolism--2011. *Molecular systems biology* **7**, 535, doi:10.1038/msb.2011.65 (2011).

51 Hucka, M. *et al.* The systems biology markup language (SBML): a medium for representation and exchange of biochemical network models. *Bioinformatics* **19**, 524-531, doi:10.1093/bioinformatics/btg015 (2003).

52 Govantes, F. *et al.* Regulation of the atrazine-degradative genes in Pseudomonas sp. strain ADP. *FEMS microbiology letters* **310**, 1-8, doi:10.1111/j.1574-6968.2010.01991.x (2010).

53 Guo, Q., Zhang, J., Wan, R. & Xie, S. Impacts of carbon sources on simazine biodegradation by Arthrobacter strain SD3-25 in liquid culture and soil microcosm. *International Biodeterioration & Biodegradation* **89**, 1-6 (2014).

54 Dsouza, M., Taylor, M. W., Turner, S. J. & Aislabie, J. Genomic and phenotypic insights into the ecology of Arthrobacter from Antarctic soils. *BMC Genomics* **16**, 36, doi:10.1186/s12864-015-1220-2 (2015).

55 Deutch, C. E. L-Proline catabolism by the high G + C Gram-positive bacterium Paenarthrobacter aurescens strain TC1. *Antonie Van Leeuwenhoek* **112**, 237-251, doi:10.1007/s10482-018-1148-z (2019).

56 Mahadevan, R. & Schilling, C. H. The effects of alternate optimal solutions in constraint-based genome-scale metabolic models. *Metab Eng* **5**, 264-276 (2003).

57 Zhang, Q. *et al.* Impacts of nitrogen and phosphorus on atrazine-contaminated soil remediation and detoxification by Arthrobacter sp. strain HB-5. *Environmental earth sciences* **71**, 1465-1471 (2014).

58 Zhang, C., Li, Y., Wang, C., Niu, L. & Cai, W. Occurrence of endocrine disrupting compounds in aqueous environment and their bacterial degradation: A review. *Critical Reviews in Environmental Science and Technology* **46**, 1-59, doi:10.1080/10643389.2015.1061881 (2015).

59 Meyer, F. *et al.* The metagenomics RAST server – a public resource for the automatic phylogenetic and functional analysis of metagenomes. *BMC Bioinformatics* **9**, 1-8, doi:10.1186/1471-2105-9-386 (2008).

60 Orth, J. D., Thiele, I. & Palsson, B. O. What is flux balance analysis? *Nat Biotech* **28**, 245-248, doi:http://www.nature.com/nbt/journal/v28/n3/abs/nbt.1614.html#supplementary-information (2010).

61 Varma, A. & Palsson, B. O. Stoichiometric flux balance models quantitatively predict growth and metabolic by-product secretion in wild-type Escherichia coli W3110. *Applied and environmental microbiology* **60**, 3724-3731 (1994).

62 Thiele, I. & Palsson, B. O. A protocol for generating a high-quality genome-scale metabolic reconstruction. *Nat Protoc* **5**, 93-121, doi:10.1038/nprot.2009.203 (2010).

63 Harcombe, W. R. *et al.* Metabolic resource allocation in individual microbes determines ecosystem interactions and spatial dynamics. *Cell reports* **7**, 1104-1115, doi:10.1016/j.celrep.2014.03.070 (2014).

64 King, Z. A. *et al.* Escher: A Web Application for Building, Sharing, and Embedding Data-Rich Visualizations of Biological Pathways. *PLoS computational biology* **11**, e1004321, doi:10.1371/journal.pcbi.1004321 (2015).

Acknowledgments

This work was funded by grants from the NSFC-ISF joint program (31461143009), Israel Science Foundation Grant no. 1416/14. Atrazine was a gift of Agan Adama (Ashdod, Israel). We thank Omer Kapiluto for statistical support.

598 **Author Contributions**

599 S.O, R.Z, T.L and S.F designed the study, constructed the model and performed *in*
600 *silico* analysis. Z.R, S.P, R.A, and D.G designed and performed the *in vitro*
601 experiments. Y.K and H.E analyzed and reviewed the results. All authors and
602 approved the final version of the manuscript.

603

604 **Additional Information**

605 Supplementary information:

606 Supplemental data 1 – Model reactions and metabolites

607 Supplemental data 2 – SBML model file

608 Supplemental data 3 – Simulation parameters and defaults.

609 Supplemental data 4 – Alternative media compositions

610 Supplemental data 5 – Supplemental figures

611 Competing Interests:

612 The authors declare that they have no conflict of interest.

613

614 **FIGURE LEGENDS**

615

616 Figure 1. Atrazine metabolism as implemented in the cytoplasm compartment of *P.*
617 *aurescens* TC1 genome scale metabolic model reconstruction (*i*RZ1176). External
618 metabolites are notated with an e0;
619
620 Figure 2. Growth performances of *P.aurescens* TC1 in dependence on the availability
621 of different carbon and nitrogen sources. (A) Predicted and observed *A.aurescens* TC1
622 growth in mineral minimal media supplemented with Atrazine or its degradation
623 intermediates. ATZ-Atrazine, NH4, GLU-Glucose, ETH - Ethylamine, ISO –
624 Isopropylamine, CTRL - control. Values are normalized by dividing in maximal value.
625 (B) Surface plot rendering *P.aurescens* TC1 growth (biomass) in dependence on
626 atrazine, glucose and NH4 availability. Color scale is indicative of biomass (Z-axis).
627
628 Figure 3. Predicted and observed growth performances of *P. aurescens* TC1 growth in
629 mineral minimal media with glucose complemented by different amino acids and
630 atrazine. ATZ-Atrazine, HIS- Histdine, ILE-Isoluecine and MET- Metionine. Observed
631 values represents mean in triplicates; bars represent SD.
632
633 Figure 4. Predicted and observed atrazine degradation in modified media. High and
634 low phosphate concentrations: 50 and 15 mmol/gdw h for predicted and 0.081 and
635 0.081 g/l for observed, respectively. ATZ- atrazine, GLU- glucose. Observed values
636 represents mean in triplicates; bars represent SD.
637

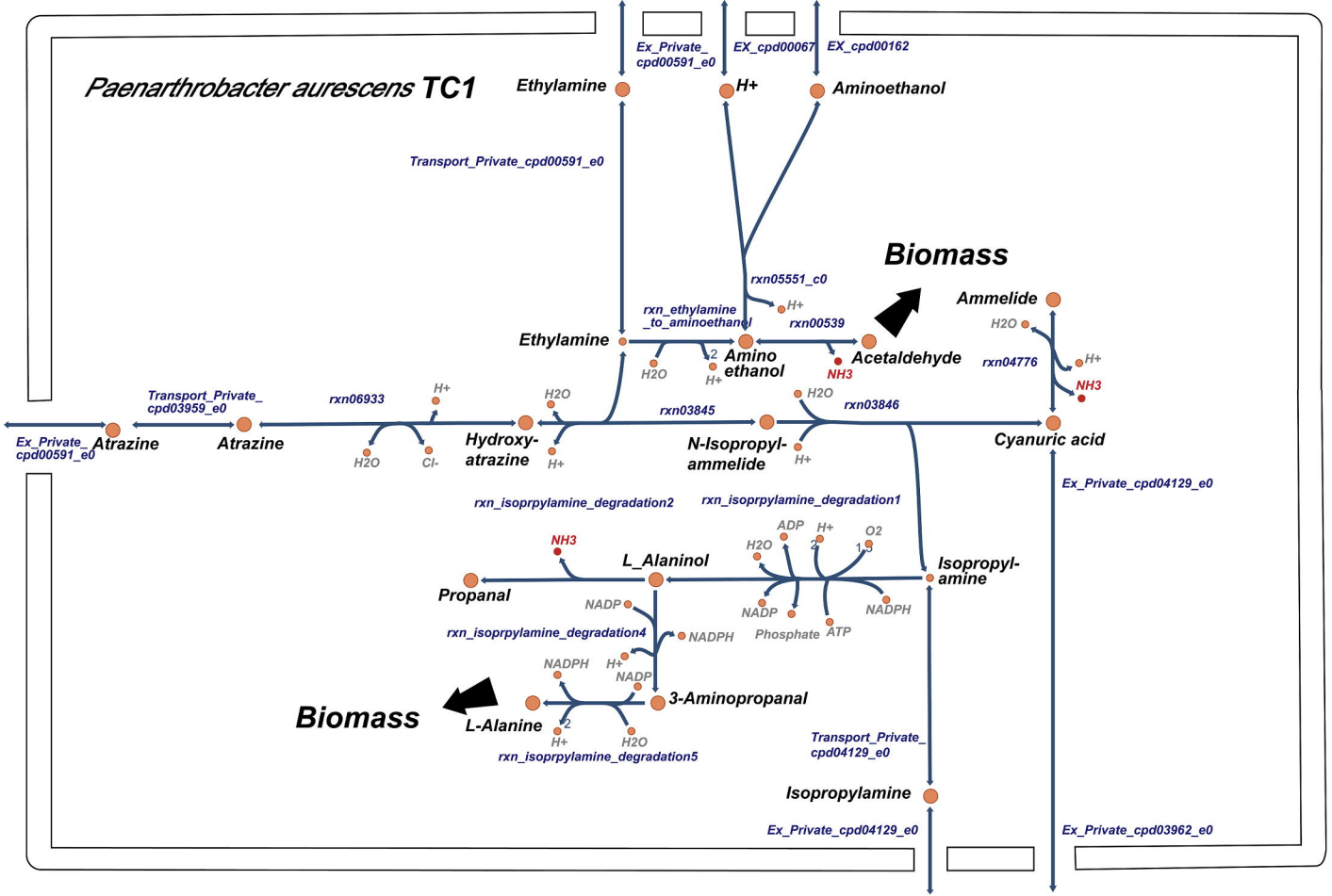
Paenarthrobacter aurescens TC1
Ex_Private_ cpd00591_e0
EX_cpd00067
EX_cpd00162
Ethylamine
H+
Aminoethanol
Transport_Private_cpd00591_e0
Biomass
rxn05551_c0
H+
Ammelide
rxn_ethylamine _to_aminoethanol
rxn00539
Ethylamine
Amino ethanol
Acetaldehyde
H2O
2
H+
NH3
H2O
rxn04776
H+
NH3
Transport_Private_ cpd03959_e0
rxn06933
H+
H2O
rxn03845
H2O
rxn03846
Ex_Private_ cpd00591_e0
Atrazine
Atrazine
H2O
Cl-
Hydroxy- atrazine
H+
N-Isopropyl- ammelide
H+
Cyanuric acid
Ex_Private_cpd04129_e0
rxn_isoprpylamine_degradation2
rxn_isoprpylamine_degradation1
ADP
H+
O2
NH3
H2O
2
1
3
L_Alaninol
Isopropyl- amine
Propanal
NADP
NADP
NADPH
rxn_isoprpylamine_degradation4
NADPH
Phosphate
ATP
NADPH
H+
NADP
3-Aminopropanal
Biomass
L-Alanine
2
H+
H2O
rxn_isoprpylamine_degradation5
Transport_Private_ cpd04129_e0
Isopropylamine
Ex_Private_cpd04129_e0
Ex_Private_cpd03962_e0

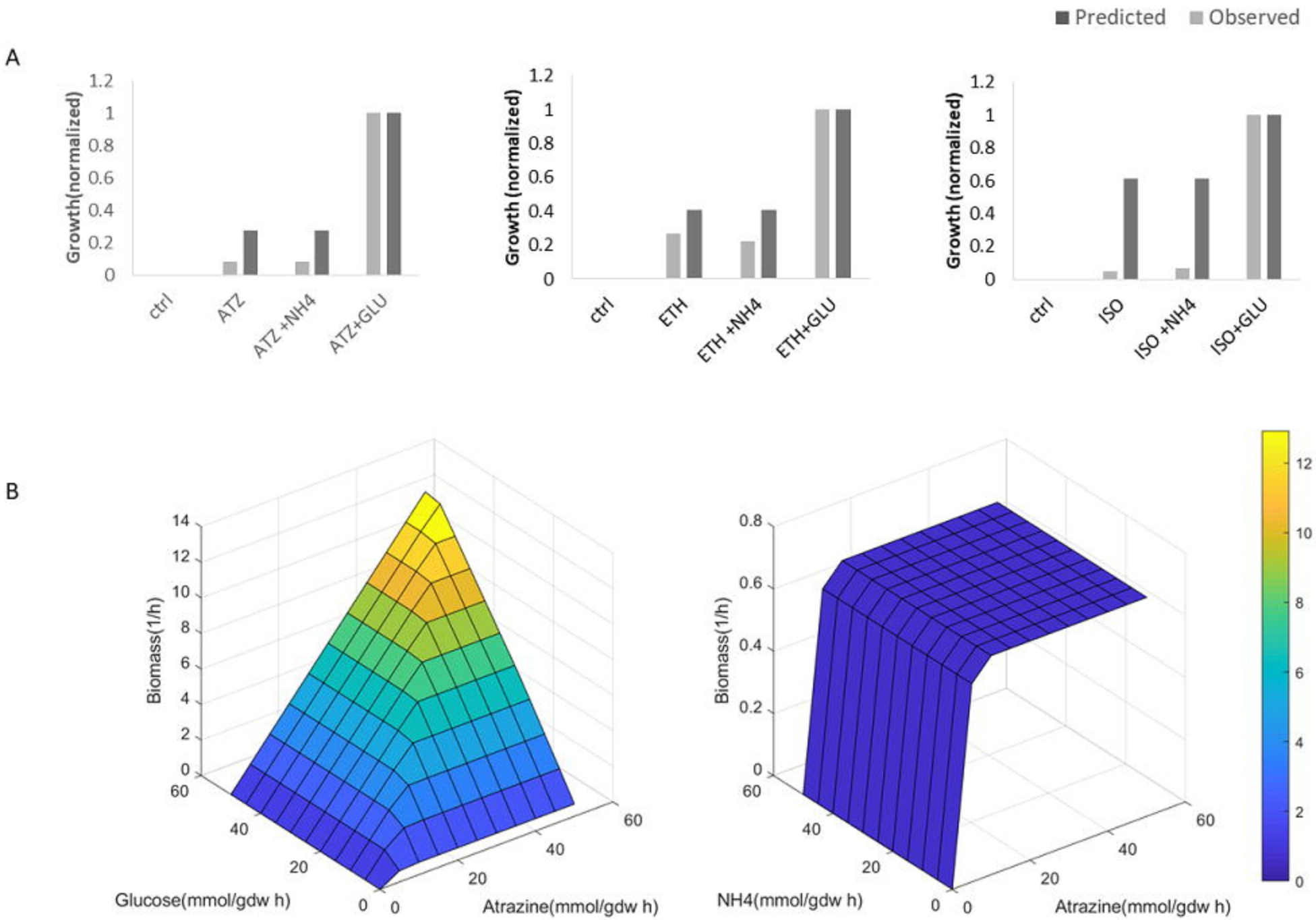
Predicted
Observed
A
Growth(normalized)
1.2
1
0.8
0.6
0.4
0.2
0
ctrl
ATZ
ATZ +NH4
ATZ+GLU
Growth (normalized)
ETH
ETH +NH4
ETH+GLU
ISO
ISO +NH4
ISO+GLU
B
Biomass(1/h)
Glucose(mmol/gdw h)
Atrazine(mmol/gdw h)
NH4(mmol/gdw h)

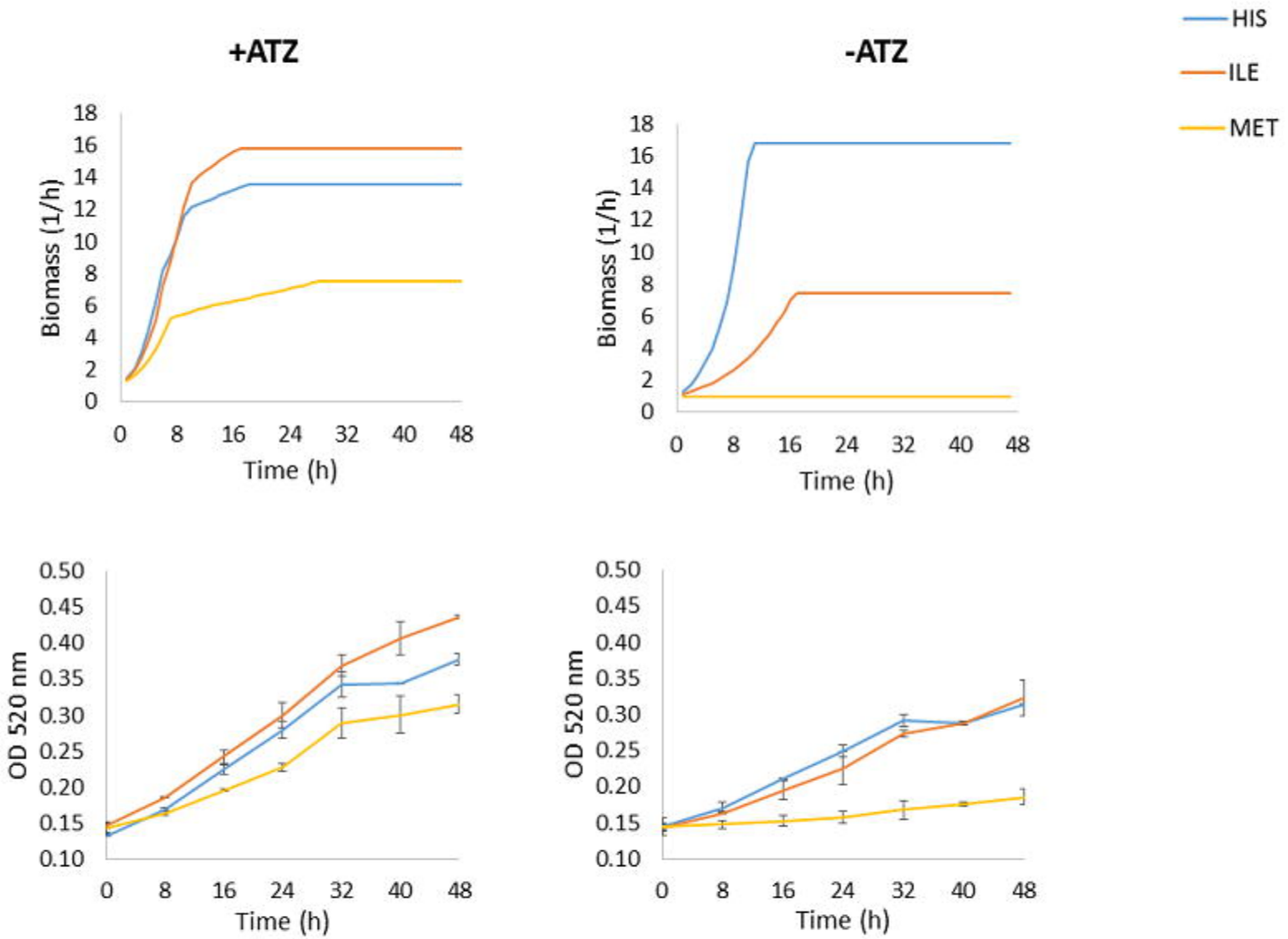
+ATZ
-ATZ
HIS
ILE
MET
Biomass (1/h)
Time (h)
OD 520 nm
0
2
4
6
8
10
12
14
16
18
0.10
0.15
0.20
0.25
0.30
0.35
0.40
0.45
0.50
0
8
16
24
32
40
48

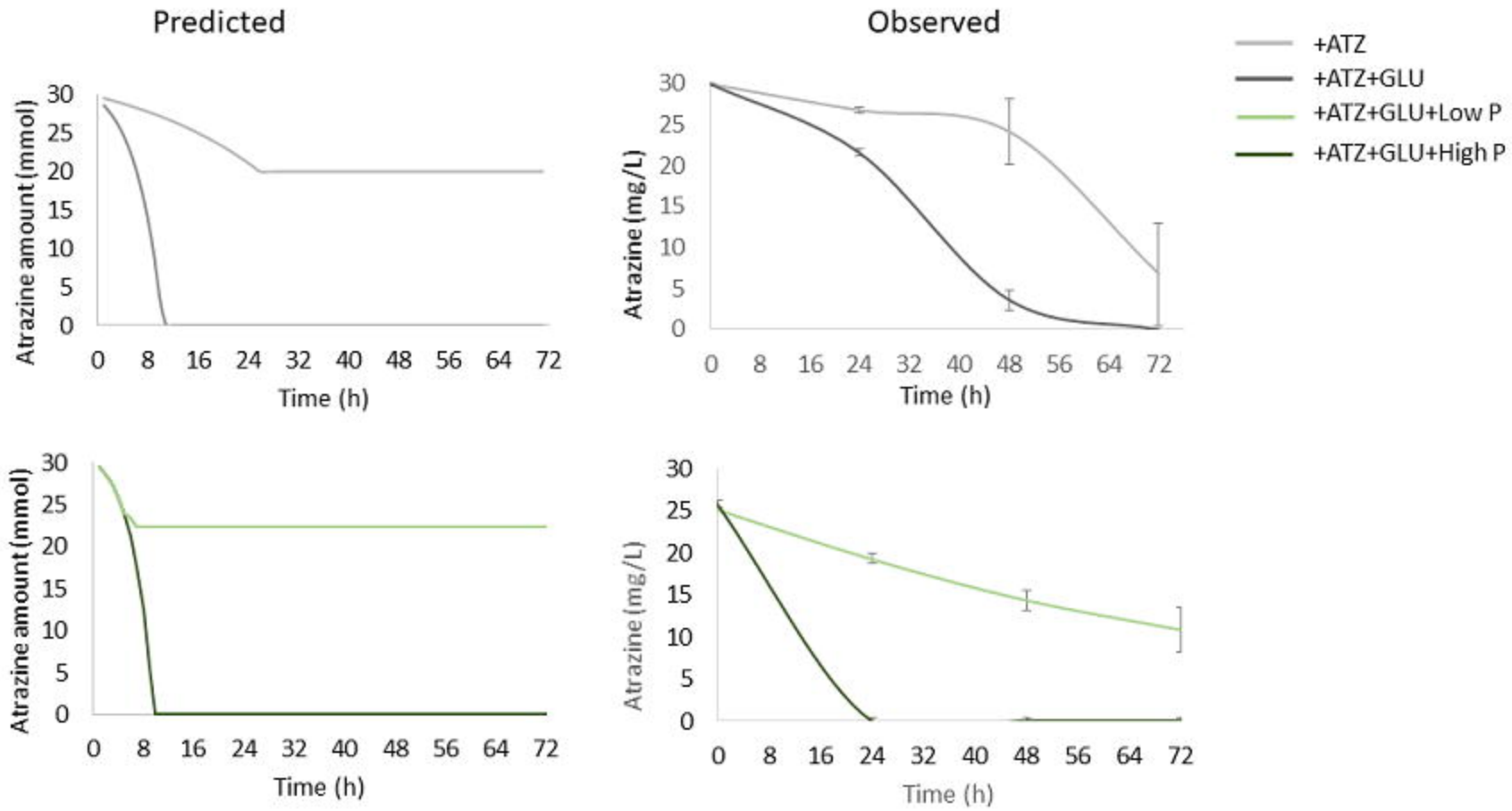
Predicted
Observed
+ATZ
+ATZ+GLU
+ATZ+GLU+Low P
+ATZ+GLU+High P
Atrazine amount (mmol)
Atrazine (mg/L)
Time (h)
0
5
10
15
20
25
30
0
8
16
24
32
40
48
56
64
72